Characterization of Chemical Bonds in Bimetallic Cyanides Using X-ray Absorption Spectroscopy at $L_{2,3}$ Edges

M.-A. Arrio,*,† Ph. Sainctavit,†,‡ Ch. Cartier dit Moulin,‡ T. Mallah,§ M. Verdaguer,§ E. Pellegrin,⊥ and C. T. Chen⊥

Contribution from the Laboratoire de Minéralogie-Cristallographie, CNRS URA9, Universités Paris 6 et 7, 4 place Jussieu, 75252 Paris Cedex 05, France, Laboratoire pour l'Utilisation du Rayonnement Electromagnétique, CNRS-CEA-MENJS UMR 130, Bât 209d, 91405 Orsay Cedex, France, Laboratoire de Chimie des Métaux de Transition, CNRS URA 419, Université Paris 6, 4 place Jussieu, 75252 Paris Cedex 05, France, and AT&T Bell Laboratories, Murray Hill, New Jersey 07974

Received December 21, 1995[⊗]

Abstract: X-ray absorption spectroscopy at the $L_{2,3}$ edges of 3d transition metals has been used to study the electronic structure of molecular-based magnets with Curie temperatures ranging from 66 to 315 K. These magnets are bimetallic cyanides of the Prussian blue family, constructed by a three-dimensional assembling of $-NC-Cr^{III}-CN-A^{II}-$ units. The chemical selectivity of X-ray absorption spectroscopy allows information to be extracted on each of the two different metal transition ions that carry the spin moments. Using Ligand Field Multiplet calculations, where hybridization is mainly taken into account through configuration interaction, we have been able to reproduce nicely all the features of the divalent 3d ion $L_{2,3}$ edges. From the knowledge of the exact ground state, we have determined its electronic structure and relevant parameters, such as the crystal field strength and the spin−orbit coupling. We have separated covalence and charge transfer effects occurring in the bond between the 3d ions and the cyano ligand. From the $L_{2,3}$ edges of A^{II} divalent ions, we found that the $A^{II}-NC$ bond has a weak covalent character with a 10% charge transfer. From the $L_{2,3}$ edges of Cr^{III}, where Cr ions are bonded to the carbon atom of the cyano ligand, we have shown that the Ligand Field Multiplet model is still fully applicable for strongly hybridized bonds. In this case it is essential to separate between covalence and charge transfer and to take the charge transfer into account through π back-bonding. The precise knowledge of these parameters is essential for the determination of macroscopic characters like magnetic properties.

Introduction

Long-range magnetic ordering at high temperature has been extensively pursued in synthetic molecular based magnets over the last ten years.[1−10] Recently, high T_c molecular based magnets have been obtained by Gadet et al.[3,5] These compounds are bimetallic cyanides derived from Prussian Blue by mixing the molecular complex $[Cr(CN)_6]^{3-}$ with paramagnetic divalent 3d transition metal cations A^{II}.[2−7] One-to-one $Cs[A^{II}Cr^{III}(CN)_6]\cdot xH_2O$ or two-to-three $A^{II}_3[Cr^{III}(CN)_6]_2\cdot x'H_2O$ stoichiometry may be obtained depending on the nature of the countercation of the hexacyanochromate(III) precursor. The octahedral geometry of the $[Cr(CN)_6]^{3-}$ precursor, the ability of the nitrogen atoms to substitute the water molecules coordinated to the A^{II} ion, and the $-Cr-CN-A^{II}-$ linear linkage lead to a three-dimensional network. The long-range order results from short-range exchange interaction between the spin-carriers through the cyanide bridge. Indeed, the cyanide bridge has been shown to be a good mediation for the electronic interaction between two paramagnetic metal ions.[6] By changing transition metal cations A^{II} (A^{II} can be Mn^{II}, Fe^{II}, Co^{II}, or Ni^{II}), ferro- or ferrimagnetic ordering occurs below critical temperatures that range from 66 to 315 K.[7]

With the recent development of highly-resolved low-energy monochromators,[11,12] X-ray absorption spectroscopy (XAS) at $L_{2,3}$ edges has been extensively used to study 3d transition metal compounds. The transition metal $L_{2,3}$ edges correspond to the electric dipole transitions from the 2p core level to essentially the empty 3d levels (the transition is $2p^63d^n \rightarrow 2p^53d^{n+1}$ for an isolated ion) and also to a lesser extent toward the 4s levels. Transition metal $L_{2,3}$-edges absorption spectroscopy gives information about the 3d levels which are directly involved in the exchange interaction. Analysis of the $L_{2,3}$ absorption spectrum of transition metals provides information about the oxidation state, spin state, site symmetry, and crystal field splitting of the absorbing transition metal.[13−16] The application of $L_{2,3}$-edges spectroscopy has been discussed in large scientific

† Laboratoire de Minéralogie-Cristallographie, CNRS URA9.
‡ Laboratoire pour l'Utilisation du Rayonnement Electromagnétique, CNRS-CEA-MENJS UMR 130.
§ Laboratoire de Chimie des Métaux de Transition, CNRS URA 419.
⊥ AT&T Bell Laboratories.
⊗ Abstract published in *Advance ACS Abstracts,* June 15, 1996.

(1) Allemand, P. M.; Khemani, K. C.; Koch, A.; Holczer, K.; Donovan, S.; Grüner, G.; Thomson, J. D. *Science* **1991**, *253*, 301−303.
(2) *Molecular Magnetic Material*; Gatteschi, D., Kahn, O., Miller, J. S., Palacio, F., Eds.; NATO ASI Series, Series E; Kluwer: Dordrecht, The Netherlands, 1991; Vol. 198.
(3) Gadet, V.; Mallah, T.; Castro, I.; Veillet, P.; Verdaguer, M. *J. Am. Chem. Soc.* **1992**, *114*, 9213−9214.
(4) Gadet, V. Ph.D. Thesis, Université Pierre et Marie Curie, Paris, 1992.
(5) Mallah, T.; Thiébaut, S.; Verdaguer, M.; Veillet, P. *Science* **1993**, *262*, 1554−1557.
(6) Mallah, T.; Auberger, C.; Verdaguer, M.; Veillet, P. *J. Chem. Soc., Chem. Commun.* **1995**, *1*, 61−62.
(7) Ferlay, S.; Mallah, T.; Ouahès, R.; Veillet, P.; Verdaguer, M. *Nature* **1995**, *378*, 701−703.
(8) Manriquez, J. M.; Yee, G. T.; McLean, R. S.; Epstein, A. J.; Miller, J. S. *Science* **1991**, *252*, 1415−1417.
(9) Miller, J. S.; Epstein, A. J. *Angew. Chem.* **1994**, *33*, 385−415.
(10) Stumpf, H. O.; Ouahab, L.; Pei, Y.; Grandjean, D.; Kahn, O. *Science* **1993**, *261*, 447−449.
(11) Chen, C. T.; Sette, F. *Phys. Scr.* **1990**, *31*, 119−126.
(12) Sainctavit, Ph.; Lefebvre, D.; Arrio, M.-A.; Cartier dit Moulin, Ch.; Kappler, J.-P.; Schillé, J.-P.; Krill, G.; Brouder, Ch.; Mallah, T. *Jpn. J. Appl. Phys.* **1993**, *32*, 295−298.
(13) van der Laan, G.; Kirkman, I. W. *J. Phys.* **1992**, *4*, 4189−4204.

S0002-7863(95)04269-7 CCC: $12.00

domains like chemistry,[17−19] biology,[20,21] and mineralogy.[22,23] More recently $L_{2,3}$-edges spectroscopy has been used to characterize bonds in solids.[24,25]

In this paper we present isotropic $L_{2,3}$ edges of the transition metal ions for the following molecular-based magnets: $Cs[Ni^{II}Cr^{III}(CN)_6]\cdot 2H_2O$, $Co^{II}_3[Cr^{III}(CN)_6]_2\cdot 12H_2O$, $Fe^{II}_3[Cr^{III}(CN)_6]_2\cdot 18H_2O$, and $Cs[Mn^{II}Cr^{III}(CN)_6]\cdot 2H_2O$. By definition an isotropic spectrum is that resulting from the average of spectra registered with photon polarization ϵ that varies over 4π steradians. One can easily show that in the electric dipole approximation it is equivalent to registering one spectrum with one polarization on a perfectly disordered powder. The isotropic $L_{2,3}$ edges, which present chemical and orbital selectivities, are used to investigate the electronic structures of the 3d metal ions and to characterize the nature of the metal ligand bonds. The series of compounds under study is particularly interesting since some macroscopic parameters such as the critical temperature strongly depend on the occupation number of the 3d shell. We will show that isotropic XAS is a unique tool for giving precise insight into the nature of the metal−ligand bonds for molecular complexes: covalence versus ionicity, charge transfer between 3d ion and its ligands, high spin versus low spin states, or "real" versus formal ionization degree. All this information can be revealed by XAS and precisely quantified by Ligand Field Multiplet (LFM) calculations. In previous work[26] we have determined the nickel magnetic moment through X-ray Magnetic Circular Dichroism (XMCD) at Ni^{II} $L_{2,3}$ edges on $Cs[Ni^{II}Cr^{III}(CN)_6]\cdot 2H_2O$. For that, a precise analysis of the isotropic spectra, providing the necessary information on the electronic structure, was a prerequisite to quantitatively interpret XMCD data.

The main purpose of this paper is to demonstrate that isotropic XAS yields much information which can be well understood for a wide variety of compounds. Indeed, in our examples the divalent and trivalent ions are engaged in very different bonds. The divalent ions with five to eight 3d electrons are involved in slightly covalent bonds with σ-donor nitrogen atoms and with moderate crystal fields while the Cr^{III} ions are bounded to σ-donor and π-acceptor carbon atoms of the cyanide group and experience strong covalence and a large crystal field with π overlap between 3d metallic orbitals and molecular orbitals of the CN. We will show that the Ligand Field Multiplet method, already extensively applied to 3d ion $L_{2,3}$ edges in rather ionic compounds with moderate crystal fields, can also be used to describe strongly covalent ligand−metal bonds. We will point out that the calculation allows the separation of the covalence effects from charge transfer, even though both contribute to hybridization: covalence is related to the reduction of the Slater integrals while charge transfer is related to the strength and the nature of the configuration interaction. All this information can be gathered by the chemist to advance the description of the electronic structure at the atomic level and to promote understanding of the macroscopic properties of materials.

Experimental Section

Chemical Synthesis. The samples were prepared by mild chemistry methods at room temperature according to published procedures:[3,4] The molecular complex $[Cr(CN)_6]^{3-}$ is mixed with a solution of divalent cation A^{II}. In the presence of Cs^+, a cubic framework arises, $Cs^I[A^{II}Cr^{III}(CN)_6]\cdot 2H_2O$ (A/Cr stoichiometric ratio equals 1/1). The metallic cations are arranged in a rock salt structure.[3,4] Cesium ions are present in half of the tetrahedral sites of the structure as shown in the upper panel of Figure 1. Two water molecules are present per formula unit. Their location, although unknown, is assumed to be near the Cs^I ions. In the absence of Cs^I, the stoichiometry becomes A/Cr = 3/2 and the formula is $A^{II}_3[Cr^{III}(CN)_6]_2\cdot x'H_2O$. In this structure there are $[Cr(CN)_6]^{3-}$ vacancies so that one-third of the $[Cr(CN)_6]^{3-}$ groups are replaced by water molecules bonded to A^{II} ions. In both the 1/1 and the 3/2 A^{II}/Cr^{III} ratio, chromium ions are linked to six carbon atoms in octahedral symmetry. The A^{II} ion is surrounded by six nitrogen atoms in octahedral symmetry in the 1/1 compounds and, on average, by four nitrogen and two oxygen atoms (coming from water molecules) in the 3/2 compounds. The following samples have been studied: $Cs[Ni^{II}Cr^{III}(CN)_6]\cdot 2H_2O$, $Co^{II}_3[Cr^{III}(CN)_6]_2\cdot x'H_2O$, $Fe^{II}_3[Cr^{III}(CN)_6]_2\cdot yH_2O$, and $Cs[Mn^{II}Cr^{III}(CN)_6]\cdot 2H_2O$.

$L_{2,3}$-Edges XAS Experiments: Data Collection and Processing. Ni $L_{2,3}$ edges were recorded on the soft X-ray SU22 beam line of the storage ring Super-ACO at LURE (Orsay). The white beam is monochromatized by a two-beryl-crystal monochromator described elsewhere.[12,27] Co, Fe, Mn, and Cr $L_{2,3}$ edges were recorded on the U4B beam line (Dragon beam line) of the NSLS at the Brookhaven National Laboratory, where monochromatization is performed by a spherical grating.[11,28] The powder samples were pasted on a grid carved on a metal sheet. All reported spectra were measured in total electron yield detection at room temperature and under a vacuum of at least 10^{-9} mbar. For comparison with calculations, a base line was substracted by using a linear function fitted to the data below the L_3-edge region and beyond the L_2-edge region.

Ligand Field Multiplet Calculations

In order to extract quantitative information from XAS, it is necessary to simulate the spectra. The calculations are performed using the Ligand Field Multiplet Theory developed by Thole[29] in the framework established by Cowan[30] and Butler.[31] This approach takes into account all the electronic Coulomb interactions as well as the spin−orbit coupling on every shell and treats the geometrical environment of the absorbing atom through crystal field potential.[13] The spectrum is calculated as the sum of all possible transitions for an electron jumping from the 2p level toward one 3d level. No attention is paid to the electric dipole allowed 2p → 4s transitions that are experimentally and theoretically found to be negligible compared to the 2p → 3d main

(14) van der Laan, G.; Thole, B. T.; Sawatzky, G. A.; Verdaguer, M. *Phys. Rev. B* **1988**, *37*, 6587−6589.
(15) de Groot, F. M. F.; Fuggle, J. C.; Thole, B. T.; Sawatzky, A. *Phys. Rev. B* **1990**, *41*, 928−937.
(16) de Groot, F. M. F.; Fuggle, J. C.; Thole, B. T.; Sawatzky, A. *Phys. Rev. B* **1990**, *42*, 5459−5468. de Groot, F. M. F. Ph.D. Thesis, University of Nijmegen, 1991.
(17) Briois, V.; Cartier dit Moulin, C.; Sainctavit, Ph.; Brouder, C.; Flank, A.-M. *J. Am. Chem. Soc.* **1995**, *117*, 1019−1026.
(18) Cartier dit Moulin, Ch.; Rudolf, P.; Flank, A.-M.; Chen, C. T. *J. Phys. Chem.* **1992**, *96*, 6196−6198.
(19) Cramer, S. P.; de Groot, F. M. F.; Ma, Y.; Chen, C. T.; Sette, F.; Kipke, C. A.; Eichborn, D. M.; Chan, M. K.; Armstrong, W. H.; Libby, E.; Christou, G.; Brooker, S.; McKee, V.; Mullins, O. C.; Fuggle, J. C. *J. Am. Chem. Soc.* **1991**, *113*, 7937−7940.
(20) van Elp, J.; Peng, G.; Searle, B. G.; Mitra-Kirtley, S.; Huang, Y.-H.; Johnson, M. K.; Zhou, Z. H.; Adams, M. W. W.; Maroney, M. J.; Cramer, S. P. *J. Am. Chem. Soc.* **1994**, *116*, 1918−1923.
(21) George, S. J.; van Elp, J.; Chen, J.; Ma, Y.; Chen, C. T.; Park, J.-B.; Adams, M. W. W.; Searle, B. G.; de Groot, F. M. F.; Fuggle, J. C.; Cramer, S. P. *J. Am. Chem. Soc.* **1992**, *114*, 4426−4427.
(22) Cressey, G.; Henderson, C. M. B.; van der Laan, G. *Phys. Chem. Miner.* **1993**, *20*, 111−119.
(23) van der Laan, G.; Pattrick, R. A. D.; Henderson, C. M. B.; Vaughan, D. J. *J. Phys. Chem. Solids* **1992**, *53*, 1185−1190.
(24) van der Laan, G.; Zaanen, J.; Sawatzky, G. A.; Karnatak, R.; Esteva, J.-M. *Phys. Rev. B* **1986**, *33*, 4253−4263.
(25) Kotani, A.; Okada, K. *Tech. Rep. ISSP, Ser. A* **1992**, No. 2562.
(26) Arrio, M. A.; Sainctavit, Ph.; Cartier dit Moulin, Ch.; Brouder, Ch.; de Groot, F. M. F.; Mallah, T.; Verdaguer, M. *J. Phys. Chem.* **1996**, *100*, 4679−4684.
(27) Sainctavit, Ph.; Lefebvre, D.; Cartier dit Moulin, Ch.; Laffon, C.; Brouder, Ch.; Krill, G.; Schillé, J.-Ph.; Kappler, J.-P.; Goulon, J. *J. Appl. Phys.* **1992**, *72*, 1985−1988.
(28) Chen, C. T.; Sette, F. *Rev. Sci. Instrum.* **1990**, *60*, 1616−1621.
(29) Thole, B. T.; van der Laan, G.; Fuggle, J. C.; Sawatzky, G. A.; Karanatak, R. C.; Esteva, J.-M. *Phys. Rev. B* **1985**, *32*, 5107−5118.
(30) Cowan, R. D. *The Theory of Atomic Structure and Spectra*; University of California Press: Berkeley, 1981.
(31) Butler, P. H. *Point Group Symmetry, Applications, Methods and Tables*; Plenum: New York, 1991.

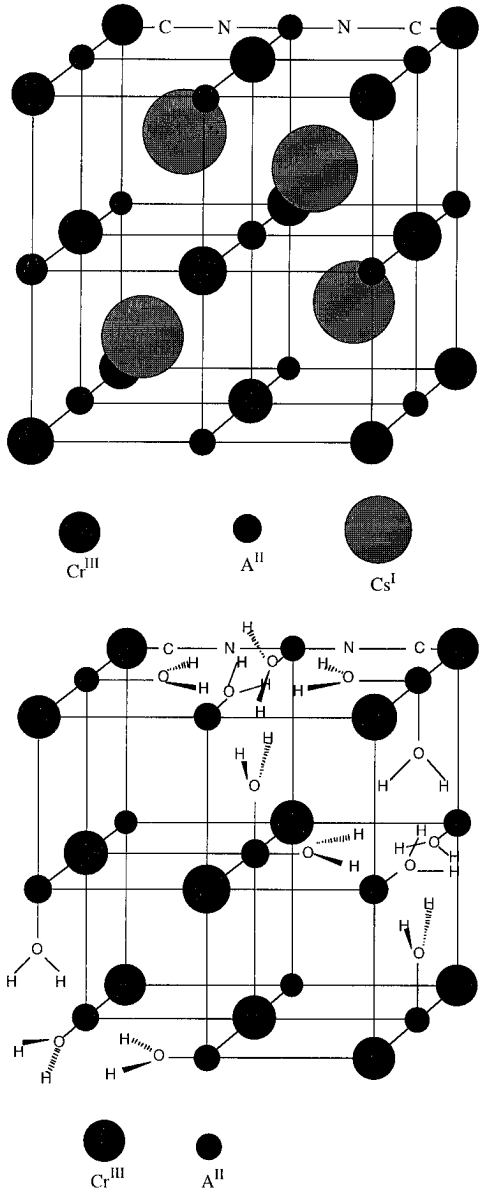

Figure 1. Upper panel: crystallographic structure of $Cs^I[A^{II}Cr^{III}(CN)_6]\cdot 2H_2O$. Cesium atoms are in the interstitial sites and water molecules are not represented. Lower panel: crystallographic structure of $A^{II}_3[Cr^{III}(CN)_6]_2\cdot xH_2O$.

channel.[32] In the simplest formulation, we attribute a pure $3d^n$ configuration to the 3d transition ions in the ground state and calculate transitions between $2p^63d^n$ ground state and $2p^53d^{n+1}$ excited states. The inter electronic repulsions are introduced through Slater integrals, F^2_{dd} and F^4_{dd} for the initial state and F^2_{dd}, F^4_{dd}, F^2_{pd}, G^1_{pd}, and G^3_{pd} for the final state. The Slater integrals are calculated through an atomic Hartree−Fock model and are scaled down by a reduction factor κ which reflects the electronic delocalization. The κ factor is comparable to the factor $\beta = B/B_0$ used in optical spectroscopy for ordering the nephelauxetic series,[33] where B_0 and B are respectively the free ion and the chemically bonded Racah parameter ($B_0 = F^2/49 - 5F^4/441$).[33] The atomic spin−orbit coupling parameters, ζ_{3d} and ζ_{2p}, are first calculated through the monoelectronic potential around the free ion. They are slightly adjusted to take into account modifications of the electronic potential by solid state effects. The octahedral surrounding of the metal ion is represented by an octahedral crystal field potential whose strength is parametrized by $10Dq$. At this point hybridization is only present through the reduction parameter κ and it is impossible to take into account the ligand−metal charge transfer. To model this effect, one has to perform the calculation with initial and final states that are mixtures of two or three appropriate configurations. This method is related to the Zaanen−Sawatzky−Allen model[24,25,34,35] except that the ligand orbitals are bound states instead of band-like states. The initial state of a $3d^n$ divalent ion is taken to be a linear combination of two configurations: $|\phi_i\rangle = \alpha|3d^n\rangle + \beta|3d^{n+1}\underline{L}\rangle$, where $3d^{n+1}$ stands for an extra 3d electron coming from the ligands and $\underline{L}$ for the corresponding hole on a ligand orbital. In the same way the final state levels are $|\phi_f\rangle = \alpha'|2p^53d^{n+1}\rangle + \beta'|2p^53d^{n+2}\underline{L}\rangle$. The charge transfer energy for the ground state is defined as $\Delta = E(3d^{n+1}\underline{L}) - E(3d^n)$, where $E(3d^{n+1}\underline{L})$ and $E(3d^n)$ are the average energies of respectively the $3d^{n+1}\underline{L}$ and $3d^n$ configurations. For the final state the charge transfer energy is defined as $\Delta' = E(2p^53d^{n+2}\underline{L}) - E(2p^53d^{n+1})$, where $E(2p^53d^{n+2}\underline{L})$ and $E(2p^53d^{n+1})$ are the average energies of respectively the $2p^53d^{n+2}\underline{L}$ and $2p^53d^{n+1}$ configurations. Δ' can be expressed in function of Δ by $\Delta' = \Delta + U_{dd} - U_{dp}$, where U_{dd} and U_{dp} are the average Coulomb interaction energies of dd and dp electron pairs.[25] The strength of the charge transfer hybridization is represented in octahedral symmetry by the two ligand−metal charge transfer integrals $V_{t_{2g}}$ and V_{eg} with $V = \langle 3d^n|H|3d^{n+1}\underline{L}\rangle$.[34]

The aim of the calculation is to compute the intensities of transitions that occur at specific energies. In order to compare them to the experimental $L_{2,3}$ spectra, the theoretical transitions must be convoluted by a broadening function that takes into account the intrinsic core-hole lifetime and the instrumental resolution.

Results and Discussion

In this section, we present the experimental and the calculated $L_{2,3}$ edges of the transition metals. We first present the A^{II} $L_{2,3}$ edges and then the Cr^{III} $L_{2,3}$ edges. The Cr^{III}−CN bond is expected to have a much stronger covalent character than the A^{II}−NC bond.

A^{II} $L_{2,3}$ Edges (A = Ni, Co, Fe, and Mn): A^{II}−NC Bond. The experimental and the calculated $L_{2,3}$-edges absorption spectra are presented in Figure 2. The experimental spectra are characteristic of A^{II} ions in high spin states. The calculations have been performed in the Ligand Field Multiplet model with hybridization by using two configurations in the initial state and in the final state. All the calculations were performed in an octahedral symmetry at 300 K. The distortions of the A^{II} site in the 3:2 compounds are weak and the symmetry can be considered as O_h. For all the A^{II} ions, a good agreement is obtained between experiment and calculation where all the manifold features due to large multiplets are reproduced. From these calculations, we deduce a precise knowledge of the multielectronic wave function that describes the ground state for each A^{II} ion. The symmetry of the ground state is defined by its O_h irreducible representation (the Γ_i^+ irreps after Butler[31]), the spin−orbit parameters for the 3d shell (ζ_{3d}) and 2p shell (ζ_{2p}), the crystal field strength ($10Dq$), and the Slater integrals reduction factor (κ). These parameters are the same for the initial and the final states and they are given in Table 1. We found a weak crystal field with $10Dq$ ranging from 0.7 to 1.15 eV depending on the divalent ion in the molecular-based magnet. The values of the crystal field parameters are in agreement with optical spectroscopy measurements that we also performed and comparable to $10Dq$ for hexacoordinated divalent 3d ions with similar ligands.[33,36]

The calculations allow the characterization of the chemical bonds of A^{II} ions with the nitrogen atoms of the cyano bridge.

(32) Bianconi, A.; Della Longa, S.; Li, C.; Pompa, M.; Congiu-Castellano, A.; Udron, D.; Flank, A. M.; Lagarde, P. *Phys. Rev. B* **1991**, *44*, 10126−10138.

(33) Lever, A. B. P. *Inorganic electronic spectroscopy*, 2nd ed.; Amsterdam: Elsevier, 1984.

(34) Zaanen, J.; Westra, C.; Sawatzky, G. A. *Phys. Rev. B* **1986**, *33*, 8060−8073.

(35) Sawatzky, G. A. *Core-Level Spectroscopy in Condensed Systems*; Springer-Verlag: Kashikojima, 1987; pp 99−133.

(36) Fisher, D. W. *J. Phys. Chem. Solids* **1971**, *32*, 2455−2480.

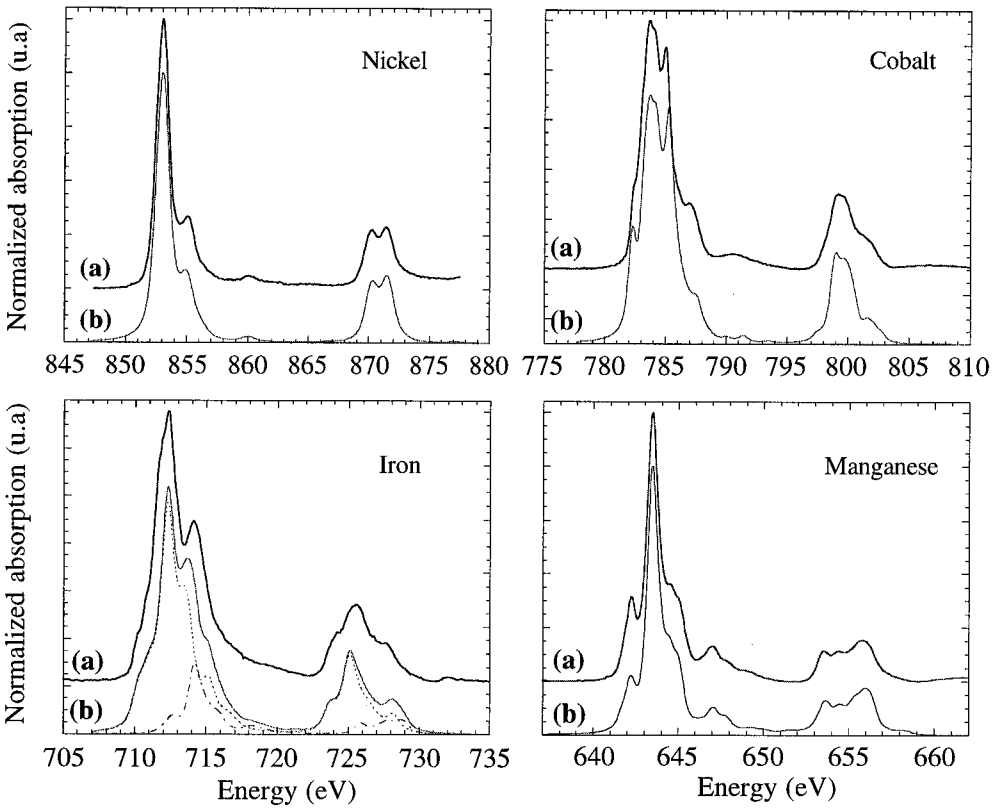

Figure 2. Experimental A^{II} $L_{2,3}$-edges spectra compared with the theoretical spectra. Top left: Ni^{II} $L_{2,3}$ edges of $Cs[Ni^{II}Cr^{III}(CN)_6]\cdot 2H_2O$. Top right: Co^{II} $L_{2,3}$ edges of $Co^{II}_3[Cr^{III}(CN)_6]_2\cdot 12H_2O$. Bottom left: Fe^{II} $L_{2,3}$ edges of $Fe^{II}_3[Cr^{III}(CN)_6]_2\cdot 18H_2O$. Theoretical spectrum calculated for $^5/_6Fe^{II}$ and $^1/_6Fe^{III}$. The Fe^{II} contribution is shown by a dashed line and the Fe^{III} by a dash−dot line. Bottom right: Mn^{II} $L_{2,3}$ edges of $Cs[Mn^{II}Cr^{III}(CN)_6]\cdot 2H_2O$.

Table 1. Spin−Orbit Coupling, Slater Reduction Factor, and Crystal Field Parameters Used for $L_{2,3}$ Edges Calculations

	ζ_{2p} (eV)	ζ_{3d} (eV)	κ	$10Dq$ (eV)
Ni^{2+}	11.45	0.10	0.90	0.9
Co^{2+}	9.75	0.022	0.90	0.7
Fe^{2+}	8.50	0.052	0.90	1.15
Mn^{2+}	7.00	0.040	0.90	0.8
Cr^{3+}	5.67	0.035	0.50	3.5

Table 2. Parameters Used for Interaction Configuration Calculations

	κ	$10Dq$ (eV)	Δ (eV)	Δ' (eV)	$V_{t_{2g}}/V_{e_g}$	n_{eff}
A^{2+}	0.90	0.8−1.15	5.3	4.3	−0.5	n+0.1
Cr^{3+}	0.50	3.5	5	4	−1.4	n−0.2

We find that for N^{II}, Co^{II}, Fe^{II}, and Mn^{II} ions the A^{II}−N chemical bonds all exhibit similar characteristics. The reduction factor κ of the Slater integrals is always 90%. The same reduction has been used by Kotani et al. to calculate the spectra of the Ni^{II} and Co^{II} dihalides,[25] and this small reduction means that the A^{II}−NC bond has a weak covalent character. This is confirmed by the fact that the Ligand Field Multiplet calculation with only one configuration for the initial and one for the final state reproduces essentially all the most intense experimental features. Interaction configuration is only required to reproduce the small intensity satellites in between the edges.[26] For instance, in the case of the Ni^{II} $L_{2,3}$ edges, the weak charge transfer is at the origin of a small satellite on the high energy side of the L_3 edge at 860 eV (Figure 2).[24,26] By adjusting Δ and Δ' parameters, this satellite can be reproduced with both correct intensity and energy position. Interaction configuration parameters are given in Table 2. Moreover from calculations at Ni^{II} $L_{2,3}$ edges, we found that the intensity of the satellite is mainly governed by the Δ' parameter while the energy position of the satellite is more related to the Δ value. For all the hybridization calculations we followed Kotani's assumption by setting $V_{t_{2g}}/V_{e_g} = -0.5$, as was done for transition metal dihalides.[25] The LFM calculations for the four divalent ions lead to similar conclusions concerning the charge transfer from the ligand. We find that each A^{II} ground state is made of approximately 90% $|3d^n\rangle$ and 10% $|3d^{n+1}\underline{L}\rangle$. The weak contribution of $|3d^{n+1}\underline{L}\rangle$ is similar to the one obtained for transition metal fluorides by Kotani et al.[25] It clearly indicates that the A^{II}−N bond experiences a very small ligand−metal charge transfer. To summarize the information that can be gained from the comparison of calculations with experiments, one can say that the A^{II}−N bond is only faintly modified by covalence ($\kappa = 90\% \pm 5\%$) and charge transfer (the ground state is an almost pure $|3d^n\rangle$ configuration with only 10% $|3d^{n+1}\underline{L}\rangle$ configuration).

The features of the spectra are a fingerprint of the oxidation state which is expected to be two for all the A^{II} ions. In the following we focus on the experimental iron $L_{2,3}$ edges. The experimental Fe $L_{2,3}$ edges in $Fe^{II}_3[Cr^{III}(CN)_6]_2\cdot 18H_2O$ are different from what can be expected for pure Fe^{II} in either high- or low-spin configuration.[17] The experiment iron L_3 edge presents a double structure; we attribute the feature at 712.3 eV to Fe^{II} but the one at 714.1 eV to the presence of Fe^{III} impurities. The $Fe^{II}_3[Cr^{III}(CN)_6]_2\cdot 18H_2O$ compound is known to be unstable. We think that some Fe^{II} ions present at the surface are oxidized to Fe^{III}. The Fe $L_{2,3}$-edges calculation was performed by taking a linear combination of theoretical Fe^{II} and Fe^{III} $L_{2,3}$ edges that nicely fitted the experimental spectrum. It can be seen from Figure 2 that the double structure in L_3 edge is well reproduced. We deduce from the calculation that the

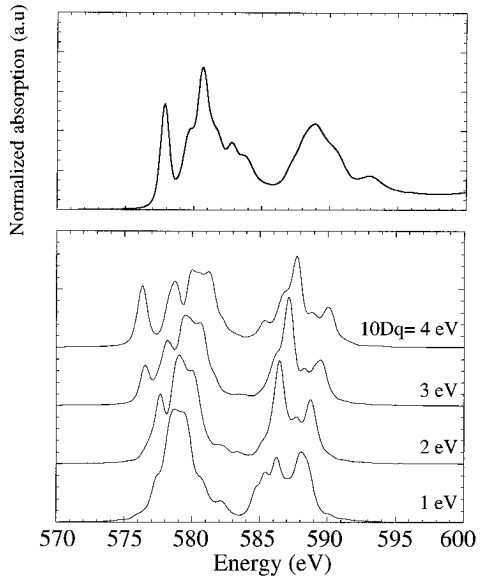

Figure 3. Upper panel: experimental Cr^{III} $L_{2,3}$-edges spectrum in $Cs^{I}Ni^{II}[Cr^{III}(CN)_6]\cdot 2H_2O$. Lower panel: theoretical spectra calculated in the LFM model for different values of 10*Dq*.

compound contains 20% of Fe^{III} on the surface in the first 50 Å.

The LFM calculation also explains the origin and the strength of the zero-field splitting in the Mn^{II} ground state. Without 3d spin−orbit coupling ($\zeta_{3d} = 0$) the Mn^{II} ground state is a pure $^6A_{1g}$ state. On the other hand, if the spin−orbit coupling is switched on but the O_h crystal field is not considered, the ground state is a pure $J = {}^5/_2$ sextuplet that is mainly built from ^6S, ^4P, and ^4G terms. The contribution of the ^{4}G term is only 0.01%. If both spin−orbit coupling and crystal field are present in the hamiltonian, the 6-fold degeneracy of the ground state is split into two irreducible representations: the 2-fold Γ_7^+ irrep and the 4-fold Γ_8^+ irrep. Indeed the spin−orbit coupling introduces the ^4G term into the ground state and, though an O_h crystal field cannot split ^6S or ^4P terms, it can split the ^4G contribution. Since the ^4G contribution is very small, one understands why the splitting between Γ_7^+ and Γ_8^+ is only ≈ 0.1 cm^{-1} for $10Dq = 0.8$ eV.

Cr^{III} $L_{2,3}$ Edges: Cr^{III}−CN Bond. The upper panel of Figure 3 shows the experimental Cr^{III} $L_{2,3}$ edges for $Cs^{I}Ni^{II}(Cr^{III}[CN]_6)\cdot 2H_2O$. The Cr^{III} $L_{2,3}$ edges of the series of bimetallic cyanides studied in this paper are all identical. This can be understood since the Cr^{III} ions have the same surroundings in the different magnets: they are bonded to six carbon atoms from the cyano ligand in octahedral symmetry. The Cr^{III} $L_{2,3}$ edges present many well-resolved features. In Figure 3, we notice the presence of a very thin and intense structure at 578 eV. This structure is followed at higher energy by a broad group of structures in which five features can be clearly identified. All the resonances from 578 to 585 eV can be attributed to the L_3 edges and the transitions above 585 eV to the L_2 edge. The energy separation between L_3 and L_2 is small and large intermixing is expected between L_3 and L_2 edges. We note that the experimental Cr^{III} spectrum of Figure 3 is much different from the $L_{2,3}$-edges spectra published for Cr^{III} in oxides.[36]

We performed LFM calculations with only one configuration for initial and final states for different strengths of the crystal field ($1 \le 10Dq \le 4$ eV) and with a constant $\kappa = 90\% \pm 5\%$. The theoretical spectra (lower panel of Figure 3) are compared to the experimental spectrum (upper panel of Figure 3). The cyano bond through carbon atoms is strongly covalent and is

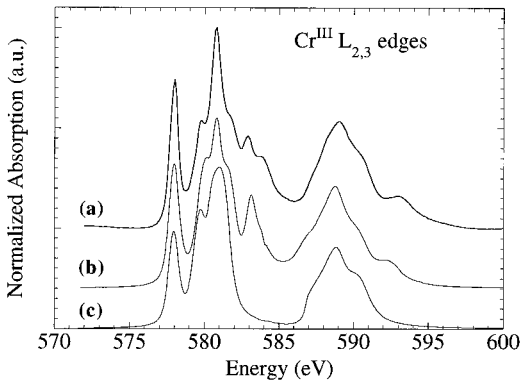

Figure 4. (a) Experimental Cr^{III} $L_{2,3}$-edges spectrum. (b) Theoretical Cr^{III} $L_{2,3}$-edges spectrum calculated with the d^3-d^2L interaction configuration. (c) Theoretical Cr^{III} $L_{2,3}$-edges spectrum calculated with $10Dq = 3.5$ eV and $\kappa = 0.5$ and no configuration interaction.

associated with a large crystal field.[33,37,38] From optical spectroscopy measurements on the molecular-based magnets we find $10Dq = 3.5$ eV for the crystal field parameter related to chromium ions. As can be seen from Figure 3, the theoretical spectra are much different from the experimental spectrum for either small or large 10*Dq*. That means that calculations based only on one configuration are not able to fit the experimental data. From the calculation with $10Dq \approx 4$ eV, one sees that a sharp resonance at 576 eV is present that can be put in correspondence with the experimental resonance at 578 eV. However, the calculated structure is at too low energy compared to the main L_3 edge. As a first step, one can consider that this sharp feature is mainly due to the strong crystal field.

We attribute the large differences between the one-configuration calculation and the experimental spectrum either to strong covalence and/or to charge transfer with the CN bond. In the case of the weak covalent A^{II}−NC bond we saw that $\kappa = 90\% \pm 5\%$ is a good estimate of the delocalization. For the Cr^{III}−CN bond, κ has to be decreased in order to take into account covalence as can be expected from nephelauxetic series.[33] Figure 4 shows the results of a one-configuration calculation with $10Dq = 3.5$ eV and a Slater reduction factor $\kappa = 0.5 \pm 0.05$ (line c). The theoretical spectrum has many fewer features than the experimental one but the low energy thin structure at L_3 edge is in better agreement with the experiment. It lies at the correct energy position compared to the main L_3 edge and has the correct intensity. This calculation confirms that the low-energy thin structure at the L_3 edge is mainly due to the strong crystal field effect and that its intensity is enhanced by the reduction of the Slater integrals that tend to reduce the energy spread of the transitions present in the peak. The strong reduction factor of the Slater integral is related to the strong covalent character of the cyano bond. The electronic delocalization induces a decrease of the local electronic repulsions on the transition metal ion. Hence Slater integrals which represent electronic repulsions have to be substantially reduced.

Reducing the Slater integrals leads to better agreement between calculation and experiment although many experimental features are still not reproduced. LFM calculation with configuration interaction has to be introduced to take into account the ligand−metal and metal−ligand charge transfers that are

(37) Balhausen, C. *Introduction to Ligand Field Theory*; McGraw-Hill: New York, 1962.
(38) Burns, R. G. *Mineralogical Applications of Crystal Field Theory*, 2nd ed.; Cambridge University Press: Cambridge, UK, 1993.
(39) Figgis, B. N.; Forsyth, J. B.; Reynolds, P. A. *Inorg. Chem.* **1987**, *26*, 101−105.
(40) Figgis, B. N.; Kucharski, E. S.; Vrtis, M. *J. Am. Chem. Soc.* **1993**, *115*, 176−181.

appropriate to the description of the $Cr^{III}-CN$ bond. Usually LFM calculations are performed with ligand-to-metal charge transfer since the admixed configuration is $|3d^{n+1}\underline{L}\rangle$. By adding this configuration we simulate a ligand-to-metal charge transfer.[25,41] This approach is not well suited to the $Cr^{III}-CN$ bond since one expects that the main charge transfer is from metal Cr^{III} toward ligand CN. Polarized neutron diffraction experiments on $K_3[Cr^{III}(CN)_6]$ have shown that the Cr^{III} ions have less than three electrons in the 3d shell.[39,40] To mimic this result, we model the bond by a metal-to-ligand charge transfer by mixing $|3d^3\rangle$ and $|3d^2L^1\rangle$ configurations. In such a scheme one 3d electron can be partly delocalized on the ligand orbital $|L\rangle$.[24,25,34,41].

The net charge transfer from the chromium ions toward the cyano ligands is due to the existence of a large π back-bonding. That means that the π overlap integral has to be increased relative to the σ one. In O_h symmetry π bonding only occurs between metal t_{2g} orbitals and cyano π molecular orbitals while σ bonding occurs between metal e_g orbitals and cyano σ orbitals. Since in the case of the $Cr^{III}-CN$ bond the π back-bonding is large, the t_{2g} overlap integral $V_{t_{2g}}$ has to be increased compared to the e_g overlap one V_{e_g}. Instead of the common value $V_{t_{2g}}/V_{e_g} = -0.5$ used for weak σ overlap, we have increased the ratio to $V_{t_{2g}}/V_{e_g} = -1.4$.

With the set of parameters from the previous discussion, we have calculated the theoretical spectrum reported on Figure 4 (curve b). A good agreement between calculation and experiment is now obtained. From this calculation we get insight about the precise ground state description of Cr^{III} and also about some $Cr^{III}-CN$ bond characteristics: the ground state is made up of 80% $|3d^3\rangle$ and 20% $|3d^2L^1\rangle$. The effective electron number on the 3d shell of Cr^{III} in the series of bimetallic cyanides is 2.8.

Conclusions

Transition metal $L_{2,3}$-edges X-ray absorption spectroscopy has been used to study local electronic structure and chemical bonds in molecular-based magnets from the Prussian Blue family. Owing to the chemical selectivity of X-ray absorption we have been able to compare $A^{II}-NC$ and $Cr^{III}-CN$ bonds. From the comparison with LFM calculations we have extracted quantitative information concerning the ground state of the 3d ions and the chemical bonds. We have determined parameters of interest like crystal field parameters $10Dq$, spin−orbit coupling constants on the 2p shell, ζ_{2p}, and on the 3d shell, ζ_{3d}, and the degree of delocalization of the 3d electrons through the κ parameter. We have also determined the amount of charge transfer and its nature. For weak covalent bonds such as $A^{II}-NC$, the ground state is a mixture of $|3d^n\rangle$ and $|3d^{n+1}\underline{L}\rangle$ configurations with a weight of 10% for the $|3d^{n+1}\underline{L}\rangle$ configuration. This gives an effective 3d electron number of $n+0.1$ on each A^{II} ion. For the $Cr^{III}-CN$ bond, we have shown through a step-by-step calculation that it is possible to determine the origin of the experimental features and then to reach a good agreement with the experiment. We first show that the origin of the thin resonance on the low-energy side of L_3 mainly originates from the large crystal field. Covalence that is responsible for delocalization and then a strong reduction of the Slater integrals tends to increase the intensity of this peak and wash out partially the L_3 resonances ranging from 578 to 584 eV. In order to reproduce the shoulder at 582 eV and the resonances at 583 and 584 eV, we have used a new kind of configuration interaction by mixing the two configurations $|3d^3\rangle$ and $|3d^2L^1\rangle$. These two configurations are those that describe properly the net charge transfer that is dominated in $Cr^{III}-CN$ by the π back-bonding. Even in a complicated case where a strong crystal field, large delocalization, and π charge transfer are present, we have been able to reproduce nicely the Cr^{III} $L_{2,3}$ spectrum. From the calculation, we deduce that the Cr^{III} ground state is well described by a mixture of 80% $|3d^3\rangle$ with 20% $|3d^2L^1\rangle$. The occupation of the Cr^{III} 3d shell is then 2.8 electrons.

Such quantities as the effective occupation of the 3d shell are essential in these magnetic compounds for the application of the "sum rules" that are powerful tools developed for the interpretation of XMCD experiments.[42] From the calculations, the multielectronic ground state wave function, $|gs\rangle$, with its coupled spin and orbital part is obtained. Its knowledge is required for the computation of matrix elements like orbital momentum $\langle gs|L_z|gs\rangle$, spin momentum $\langle gs|S_z|gs\rangle$, and magnetic dipole momentum $\langle gs|T_z|gs\rangle$ as well as even more complicated expressions.

Acknowledgment. We are glad to acknowledge the help provided by B. T. Thole and the encouragement of F. M. F. de Groot for this work. Christian Brouder is thanked for his constant support and enlightening discussions. We also thank Professor Christopher Landee for his careful reading of the manuscript and suggestions. This work has been supported partially by the European Union Contract from Human Capital and Mobility program (ERBCHXCT930360).

JA9542698

(41) de Groot, F. J. *Electron. Spectrosc. Relat. Phenom.* **1994**, *67*, 529−622.

(42) Carra, P.; Thole, B. T.; Altarelli, M.; Wang, X. *Phys. Rev. Lett.* **1993**, *70*, 694−697.